Shahrood University of Technology

Journal of Mining and Environment (JME)

Journal homepage: www.jme.shahroodut.ac.ir

Iranian Society of Mining Engineering (IRSME)

A New Proposed Model for Early Kick Detection in Drilling Operation Using Machine Learning

Mustafa Yasser Elgindy[1,2*], Ahmed Z. Nooh[3], and Ali M. Wahba[2]

1. Drilling and Well Services Engineer, Drilling and Well Services Department, Badr El-din Petroleum Company (BAPETCO), Cairo, Egypt.
2. Department of Petroleum Engineering, Faculty of Petroleum and Mining Engineering, Suez University, P.O.Box: 43221, Suez, Egypt
3. Egyptian Petroleum Research Institute (EPRI), Nasr City, Cairo, Egypt

Article Info

Received 18 July 2024
Received in Revised form 15 September 2024
Accepted 20 November 2024
Published online 20 November 2024

DOI: 10.22044/jme.2024.14787.2807

Keywords

Early Kick Detection
Machine Learning
Drilling Parameters
Abnormal Formation Pressure

Abstract

Kick monitoring, detection, and control are key elements to ensure safe drilling operations and avoid catastrophic blow-out incidents that can cause loss of life, equipment, and environmental damage. Conventional kick detection systems such as the pit volume totalizer and the flow in/out sensors identify the kick after a large amount of influx has been recorded on the surface. So, we aim to recognize the kick before it enters the wellbore by detecting the abnormal formation pressure once the bit penetrates the rock. This paper proposes a new machine learning model as an alternative solution using field drilling parameters such as true vertical depth, porosity, bulk density, resistivity, rate of penetration, weight on bit, rotation per minute, torque, standpipe pressure, flow rate, flowline temperature, and gas level. The data-driven models were developed using three separate algorithms: K-Nearest Neighbor, Random Forest, and XG Boost. 6022 field data points were split for training, testing, and validation processes. On average, the model using the random forest algorithm showed the highest accuracy in forecasting the formation pressure, with root mean squared error values and coefficient of determination values of 12.868 and 0.9638, respectively. Streamlit Deployment tool was used to create a user interface program to facilitate the prediction process. The program was tested using 196 field data points and recorded a high accuracy of 95%.

1. Introduction

Drilling oil and gas wells is surrounded by many challenges, and well control concerns have the highest priority for all working personnel. A kick, which is the undesired, uncontrolled flow of formation fluids into the wellbore, is the result of mud hydrostatic pressure becoming insufficient to sustain formation pressure, and this can happen during any drilling stage [1]. We can look at one of the well control incidents that took place in the Gulf of Mexico, the Deep-Water Horizon incident. Due to a well control event, the rig exploded and sank into the ocean, taking 11 lives with it. Also, 4 MMbbls spilled over the ocean in 87 days, and the incident cost $5.5 billion in account of the Clean Water Act penalty and $8.8 billion in natural resource damages [2]. So, the kick must be detected, handled, and removed from the well as early as possible to regain primary well control (i.e., mud hydrostatic pressure greater than formation pressure), and if the well control measures have not been applied, catastrophic events might happen that can result in the loss of life, equipment, and finances and cause environmental damage [3]. The main goal during a drilling operation is to constantly monitor the wellbore pressure and prevent any formation influx. So, the rig crew analyzes various parameters (surface and downhole) to recognize a kick. Therefore, sensors are widely distributed in the rig at the pump discharge, the flowline return to the shale shaker, and drilling parameters monitoring sensors [4]. Normal kick detection relies on mud volume in the mud system, and if the mud level increases in the tanks, this means that an

✉ *Corresponding author: mustafa.muel@pme.suezuni.edu.eg (M.Y. Elgindy)*

influx has occurred in the well.

Machine learning is the tool that seeks to identify a relationship among the data sets and has become a tool for increasing safety and optimizing operations Machine learning models will help in the automation of operations and can remove human error. Machine learning has been applied to various oil and gas topics such as rate of penetration prediction, interpretation of real well logging data, expected weight on bit and bit wear, and non-productive time prediction [5] [6].

The aim of this research is to use machine learning and drilling parameters from mud logging and MWD/LWD in order to recognize the kick before it enters the wellbore by detecting the abnormal formation pressure. This will allow for early detection of the kick, giving the rig crew an advantage to regain control of the well rather than waiting until the influx is in the well, detected by the conventional sensors, then dealing with it.

2. Kick Warning Signs

When formation pressure exceeds the hydrostatic pressure and the formation has good porosity (Φ) and permeability (K), a kick is expected [7]. Abnormal formation pressure and kick have warning signs that can be predicted from drilling parameters. Table 1 summarizes the abnormal formation pressure and kick warning signs.

Table 1 a summary of the abnormal formation pressure and kick warning signs.

No.	Parameter	The normal trend with depth	Change against high formation pressure
1	Rate of penetration (ROP) [8]	ROP decreases uniformly with the depth increase.	ROP increases and the formation becomes more drillable which is called a fast break.
2	Torque and Drag [9]	Normal increase of torque and drag.	Greater wall contact and friction increase more causing a greater increase in torque and drag.
3	Bulk Density [10]	Bulk density increases with depth	Density decreases against high pressures reflecting high porosity.
4	Cutting Size and Cutting Shape [11]	cuttings have rounded edges and are generally flat	long, and splintery with angular edges. Also, there is an increase in cutting quantity.
5	Trip, Connection, and Background Gases [12]	Depends on the formation and the time taken in connections.	increase while drilling abnormal formation pressure
6	Formation Resistivity [13]	The normal trend of the resistivity is to increase with depth.	resistivity decreases greatly as a result of the increased porosity and water content

3. Kick Detection Methods: Conventional, Mathematical, and Machine Learning

Conventional kick detection methods are [14]:

- Flow in and out sensors, located at the pump discharge line and return flow line, respectively [15].
- Pit Volume Totalizer (PVT), located at mud tanks [16] as shown in Figure 1.

These methods give an alarm when the flow rate or tank volume deviates from a pre-set limit value. Under any circumstances, any change in the tank level will lag behind the increased flow rate, so the increased flow rate will take some time to give a considerable observable pit level change. Thus, these methods detect the kick after its effect is on the surface, which is time-consuming [17] [4].

Mathematical models and equations were developed to calculate the formation pressure (P_f) by using D-exponent (d_c) [9]:

- **Eaton Method: applicable in sedimentary basins.**

$$P_f = \sigma_{ov} - (\sigma_{ov} - P_n) \times \left(\frac{dco}{dcn}\right)^{1.2} \quad (1)$$

P_f: formation pressure (ppg)
σ_{ov}: overburden gradient (ppg)
P_n: normal formation pressure gradient (ppg)
d_{co}: the observed value of dc at depth of interest
d_{cn}: normal trendline value of dc at depth of interest

- **Ratio Method: applicable in Clastic Limestone.**

$$P_f = P_n \times \left(\frac{dcn}{dco}\right) \quad (2)$$

The major problem with these mathematical equations is how to choose the correct normal compaction trend, especially when there is too little data. Also, there will be a continuous change in the mathematical equation in use due to the change in the rock type [18].

Machine learning (ML) is a discipline that uses a series of procedures and algorithms to analyze the data in order to recognize patterns, clusters, or trends and then extract fruitful information for data

analysis in an automated, enhanced way [19]. Machine learning is concerned with using the best features in conjunction with the best algorithm to build up a model capable of performing the required tasks [20]. Some machine learning models have been developed in order to overcome the problems associated with conventional methods. Some of the models analyze whether the alarm given by conventional methods is true or false, like [21]. Some use algorithms for kick detection and influx size estimation during drilling operations, like [22] and [15]. Table 2 shows a summary of some of the machine learning models used in kick detection.

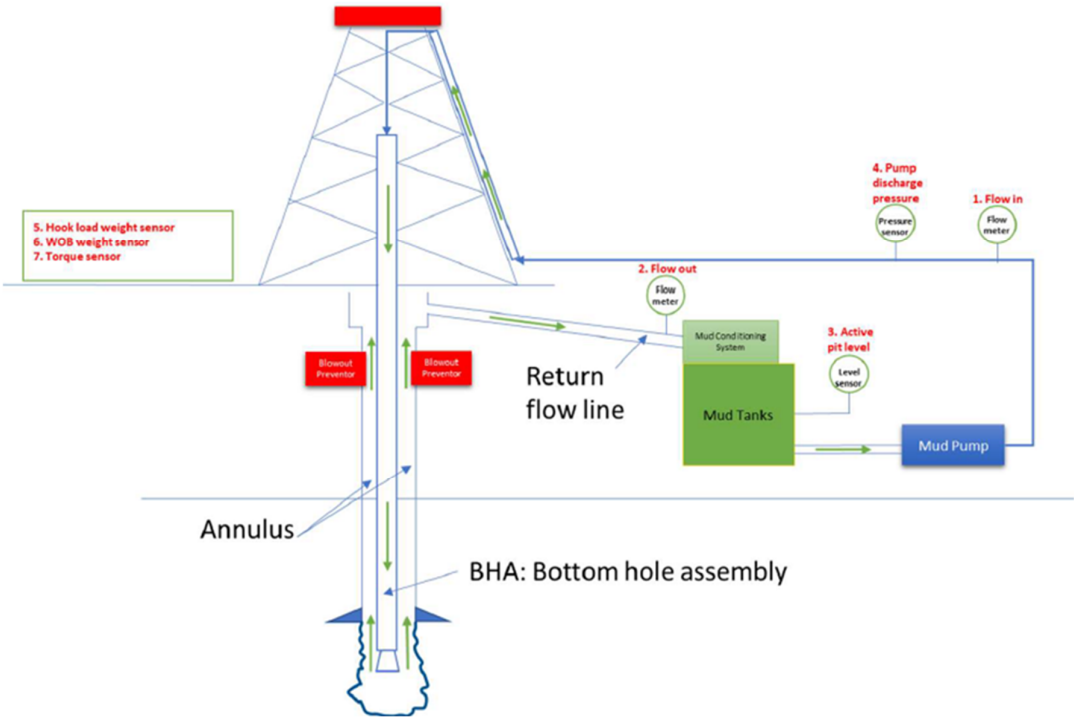

Figure 1. Drilling rig kick detection instruments and sensors locations [15]

Table 2. Summary of some of the machine learning models used in kick detection.

Model	Algorithms	Parameters	Data set	Accuracy
False alarm detection [21].	-Long short-term memory recurrent neural network (LSTM-RNN)	-D-Exponent -Standpipe pressure (SPP)	4 Cases of Kick	-
kick detection and influx size estimation during drilling operations [22]	-Long Short-Term Memory (LSTM) -Bidirectional LSTM (BiLSTM)	-Flow in/out -SPP -Choke Opening Size -Hydrostatic Pressure -Depth	Artificial Generated data set by open lab drilling simulator for an inclined well of 2500 m depth.	LSTM mud loss rate = 0.1040 kg/s over 500 epochs BiLSTM mud loss rate = 0.0744 kg/s over 500 epochs
kick detection using drilling parameters [15].	-Decision Tree - Naïve Bayes, -Logistic Regression -Neural Network	-Delta flow -Hook load -Pit volume -Weight On Bit -Rate Of Penetration -Rotation per minute (RPM) -SPP -Torque.	Artificial Generated data set by open lab drilling simulator giving 25 runs used in the mode.	Decision Tree R^2= 91.4 Naïve Bayes R^2= 78.1 Logistic Regression R^2= 61 Neural Network R^2= 70.3

4. Method and Data

Figure 2 shows the process followed to build-up the ML Model and Program.

4.1. Data Gathering

Real-time drilling parameters from mud logging, MWD/LWD, open hole logs, and repeat formation tester data (RFT) collected from 10 wells located in the Western Desert, Egypt, to be used in the Formation Pressure Prediction and Kick Detection program and model build-up. Table 3 shows the statistical summary of the input data, and the upper and lower limits of each property used in the program. 6022 points were gathered along 8.5”

holes having the following inputs:

- True Vertical Depth (TVD) (ft), Measured from MWD/LWD
- Rotation per Minute (RPM), Measured from Mud Logging and MWD/LWD
- Bit Size (in), Actual hole size being drilled
- Torque (lb. f), Measured from Mud Logging
- Porosity (%), Measured from MWD/LWD
- Standpipe pressure (Psi), Measured from Mud Logging
- Bulk Density (gm/cc), Measured from MWD/LWD
- Flow Rate (GPM), Measured from Mud Logging
- Resistivity (ohm), Measured from MWD/LWD
- Flowline Temperature (°C), Measured from Mud Logging
- ROP (M/hr.), Measured from Mud Logging and MWD/LWD
- Gas Level (PPM), Measured from Mud Logging.
- Weight on Bit (WOB) (K. lb.), Measured from Mud Logging
- Formation Pressure (Psi), Measured from RFT

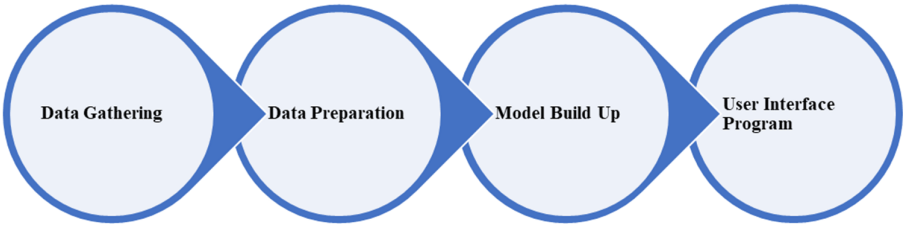

Figure 2. Model and Program Build-up Steps.

Table 3. Statistical Summary of the Input Data

Statistical Parameter	Formation Pressure	TVD	Bit Size	Porosity	Bulk Density	Resistivity	ROP	WOB	RPM	Torque	SPP	Flow In	FL Temp	Gas Level
	(Psi)	(Ft)	(in)	(%)	(gm/cc)	(ohm)	M/hr.)	(K. lb.)		(lb. f)	(psi)	(GPM)	(C)	(PPM)
Maximum	8362.22	12523.58	8.50	0.53	3.21	2000.00	149.07	55.00	213.47	14586.81	3626.72	1150.41	63.27	779334.30
Minimum	1505.24	7765.70	8.50	0.00	2.02	0.34	1.25	0.00	0.00	0.00	113.18	7.69	16.93	247.00
Range	6856.99	4757.88	8.50	0.53	1.19	1999.66	147.83	55.00	213.47	14586.81	3513.54	1142.72	46.34	779087.30
Mean	4770.24	10202.23	8.50	0.20	2.62	28.65	28.25	20.15	123.81	7491.69	2469.62	467.95	42.85	17068.01
Median	4634.14	10154.19	8.50	0.19	2.62	2.17	24.58	19.95	136.18	7391.90	2485.30	471.40	42.11	9599.26
Standard Deviation	918.20	971.85	0.00	0.11	0.11	177.15	15.90	8.99	26.54	2021.90	454.96	50.07	9.13	33675.95
1st Q	4348.59	9545.85	8.50	0.11	2.55	1.04	17.14	13.81	110.47	6084.66	2220.67	449.67	35.99	5989.52
3rd Q	5209.85	10827.35	8.50	0.28	2.69	5.22	36.55	26.75	141.13	8842.13	2722.08	498.05	47.79	16634.17

4.2. Data Preparation

The data has no missing inputs and no duplicates. So, the features and target were identified. Figure 3 shows the correlation matrix between the input data.

Data split into three trains:

- Training data set with 4335 points representing 72%.
- Test data set with 1084 points representing 18%.
- Validation data set with 603 points representing 10%.

4.3. Model Build-Up

Three different algorithms were used (KNN, Random Forest, and XG Boost) using the Python language to create the ML model. The standard parameters of each algorithm are used to create the model.

4.3.1. Machine Learning Algorithms

(1) K-Nearest Neighbors algorithm (KNN):

KNN is a non-parametric model that does not have any parameters that can be learned from the data. Also, it does not make any mathematical assumptions as it only requires [23]:

- A notion of distance from the selected point.
- An assumption that the points that are closer to one another are similar.

So, the KNN algorithm assigns a group of (K) objects in the training data set that are the closest

to a test point by using one of the similarity measures (e.g., distance function) and forecasts the required output depending on the most frequent class within the assigned K-Neighbors [24] [25].

(2) Random Forest algorithm (RF):

A ML algorithm that can solve classification and regression problems. The main element in the random forest is that for each n^{th}, a random vector (Θ_n) is generated that is independent of any previous random vectors but has the same distribution. A tree starts to expand using a training set and random vectors to result in a classifier h (x, Θ_n), where x is the input vector. After a large set of trees is generated, a vote is made for the most popular class [26] [27]. The random forest can capture the nonlinearity in the data, and this can prevent issues like high errors, high variation, and overfitting [28].

(3) XG Boost Algorithm:

Gradient boosting is an ensemble ML algorithm that combines multiple weak learners into a strong learner. XG Boost is a scalable and improved version of the gradient boosting algorithm that has higher efficiency, computational speed, and performance. XG Boost creates nodes up to the maximum depth specified and then starts pruning from backward to reduce the size of regression trees by replacing nodes that do not contribute to improving leaf classification [29] [30]. However, XGB is more likely to show overfitting as it tries to minimize the cost function values between the real and predicted features.

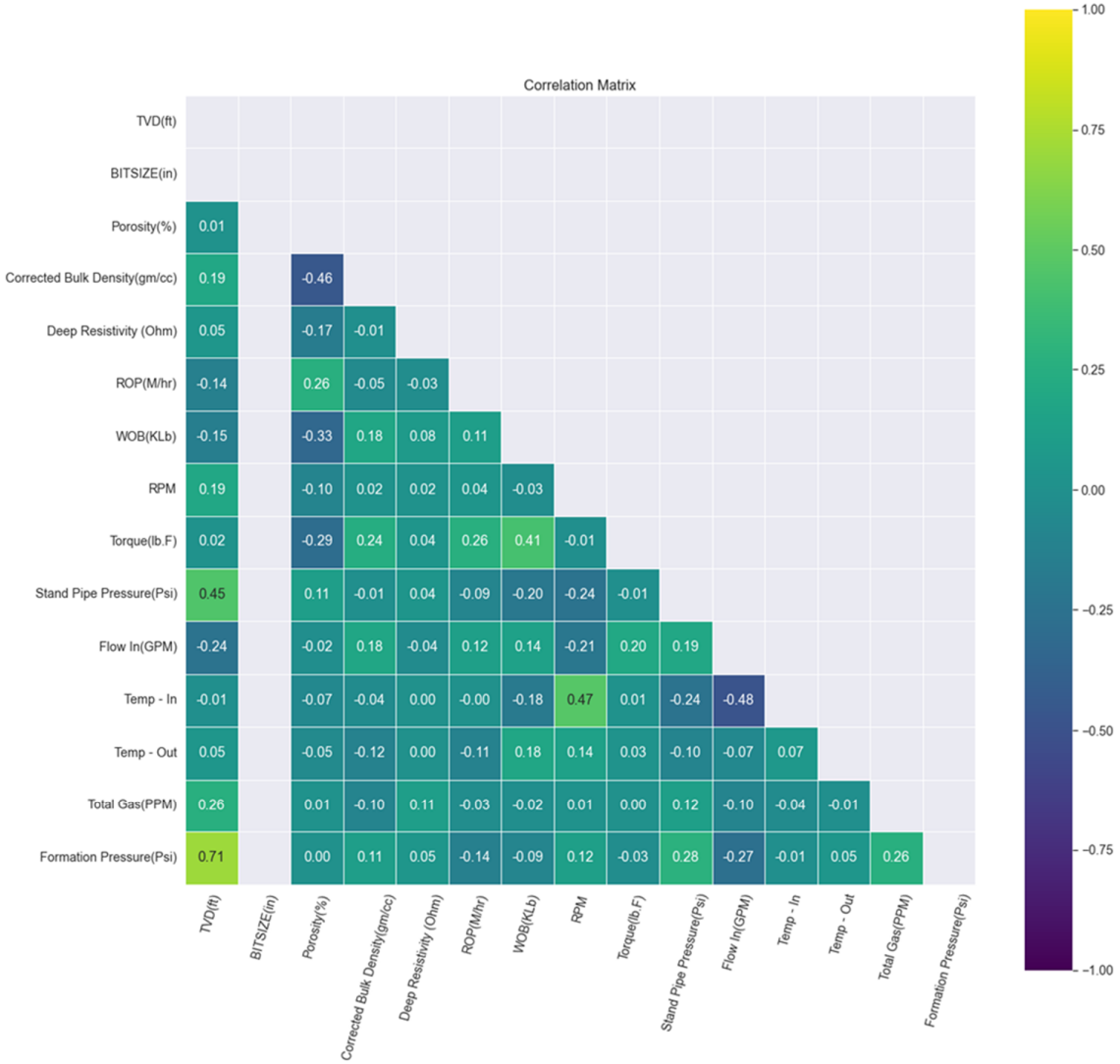

Figure 3. Correlation Matrix between the input data

4.4. Deployment and User Interface Program

It is the design solution step by putting the results obtained from the ML Model into practice. After we do the model comparison and choose the best and most competent model, we will start deploying the user interface program using **Streamlit.** The following steps are followed for deployment [31]:

- Import the chosen trained model to be able to predict based on the test data.
- Define a function so it will use the trained model for prediction inside the app.
- Create a variable to save the model prediction result and return it to the user once needed.
- Accept the input from the browser and render the model's final predictions on the web page.
- Create (n) input variables to accept the user input values from the browser.

5. Results and Discussion

5.1. Model Assessment

The use of statistical analysis of the data is a great help in evaluating the models. Root Mean Squared Error (RMSE) and Coefficient of Determination (R^2) were used as expressed in equations (3) and (4), respectively, to evaluate the models generated. Table 4 shows the results of the three models used in this paper.

$$RMSE = \sqrt{\frac{\sum_{i=1}^{n}(Formation\ Pressure_{Actual} - Formation\ Pressure_{Predicted})^2}{n}} \quad (3)$$

$$R^2 = \frac{\sum_{i=1}^{n}(Formation\ Pressure_{Actual} - Formation\ Pressure_{Predicted})^2}{\sum_{i=1}^{n}(Formation\ Pressure_{Actual} - Formation\ Pressure_{Mean})^2} \quad (4)$$

Table 4. RMSE and R-Squared of the Three Models

Model	RMSE	Average R-Squared
KNN	18.69686605	0.8343
Random Forest	12.86756387	0.9638
XG Boost	13.05530926	0.9600

Table 4 shows a comparison between the three models on RMSE and R^2 values. RMSE values show the model's accuracy, with the RMSE closer to zero corresponding to higher accuracy. R^2 values show how the actual and predicted data sets are correlated to each other, with R^2 closer to 1 being better. It can be seen that the Random Forest Model has a lower RMSE value, which means that it has higher accuracy. Also, RF shows a higher R^2 value, showing a better correlation between actual and predicted formation pressure.

Figures 4-6 show the regression plot of actual vs. predicted formation pressure for the training data set developed by KNN, RF, and XGB, respectively. Figure 4 shows a great scatter of the data and lower R^2 from the KNN model, which lowers its accuracy and gives a great variation in the predicted values from the actual values. Figure 5 shows the RF model in the training phase with a smaller scatter of the data and reasonable R^2, which is a good sign of the model. Also, it can be seen from Figure 6 and the corresponding R^2 that is very close to 1 that XGB will give accurate results in the training phase for formation pressure, but when compared with the testing and validation results, it shows a greater difference in the predicted values, which indicates overfitting of the data in this model.

Figures 7-9 represent the testing data. Figure 7 representing the KNN model in the testing phase still shows a greater scatter of the data and lower R^2 values. It can be seen from Figure 8 that there is a minimum scatter of the data and a reasonably high value of R^2 very close to the values in the training stage (Figure 5) resulting from the RF model. Figure 9 shows a lower value of R^2 in the testing phase of XGB in comparison to the extremely high value in the training phase (Figure 6).

Validation data are shown in Figures 10-12. Figure 10 of the KNN model still shows greater scatter of the data and lower R^2 values over the validation process. From Figure 11, it can be seen that the RF model maintains its correlation, accuracy, and lower scatter of the data over the three phases. Figure 12 gives good results from XGB, but this shows that the model is not stabilized over the three phases.

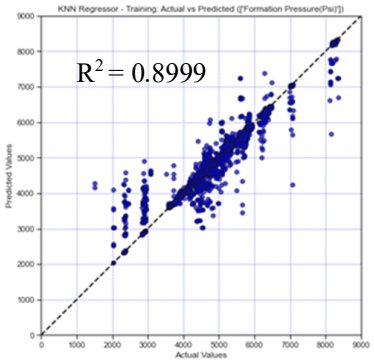

Figure 4. Regression Plot of Actual vs. Predicted Formation Pressure for KNN Model – Training Phase

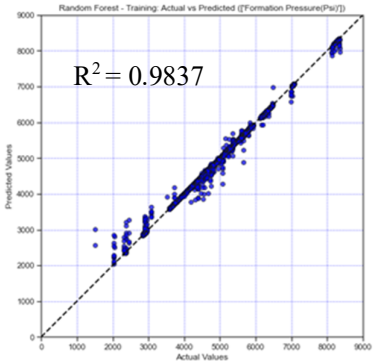

Figure 5. Regression Plot of Actual vs. Predicted Formation Pressure for RF Model – Training Phase

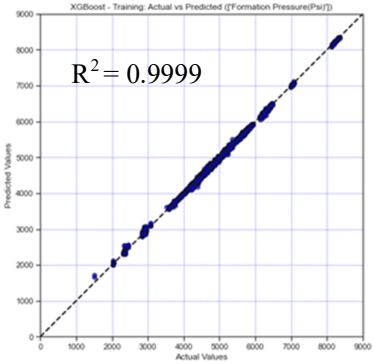

Figure 6. Regression Plot of Actual vs. Predicted Formation Pressure for XGB Model – Training Phase

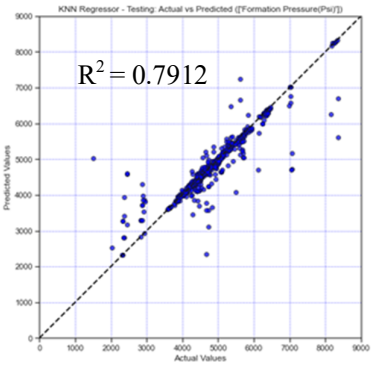

Figure 7. Regression Plot of Actual vs. Predicted Formation Pressure for KNN Model - Testing Phase

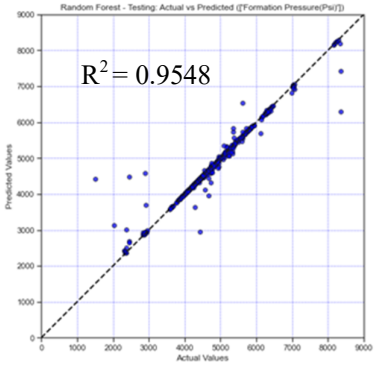

Figure 8. Regression Plot of Actual vs. Predicted Formation Pressure for RF Model - Testing Phase

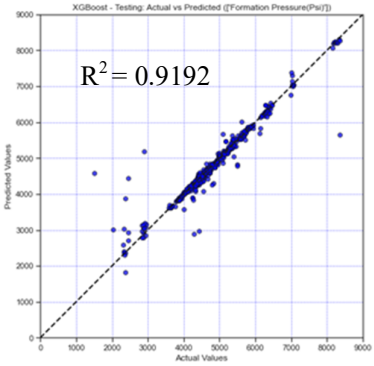

Figure 9. Regression Plot of Actual vs. Predicted Formation Pressure for XGB Model - Testing Phase

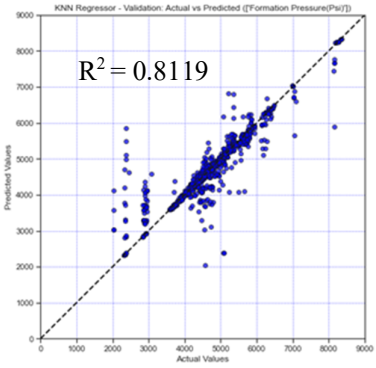

Figure 10. Regression Plot of Actual vs. Predicted Formation Pressure for KNN Model - Validation Phase

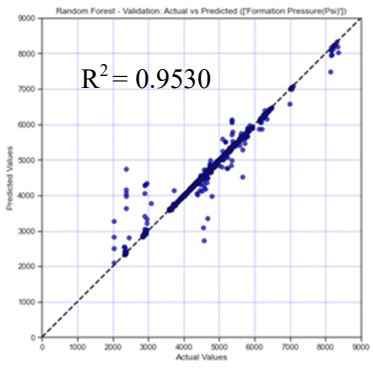

Figure 11. Regression Plot of Actual vs. Predicted Formation Pressure for RF Model - Validation Phase

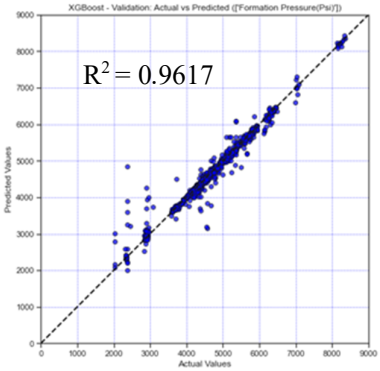

Figure 12. Regression Plot of Actual vs. Predicted Formation Pressure for XGB Model - Validation Phase

From the presented results, it can be seen that Random Forest has the best results in comparison to the other two models, as it has the lowest RMSE and higher R^2 during the testing and validation and shows no overfitting of the data during the training stage.

Well **X** is used in order to evaluate the credibility of the program. Table 5 shows a statistical summary of **X.** It can be seen that the used well data ranges in the same range as the input data. Well **X** shows the variation in pressure with depth and the sudden decrease in pressure, which

helps more to evaluate the models. A comparison of the actual and predicted formation pressure vs. depth for the KNN, RF, and XGB over a well **X** is shown in Figures 13-15, respectively. It is clear that the RF model predicts the formation pressure and the abnormal points perfectly, while KNN shows good results and XGB shows the least good, as XGB provides overfitting in the training. So, Random Forest is used to build up a user interface program.

Referring to Table 2, we can see that the presented accuracy of the random forest model in this paper is higher than the presented result of decision tree of [15]. Also, since the predicted formation pressure only depends on the immediate readings of the properties, so, there is no time delay for prediction and we will not wait for mud loss to occur like [22].

Table 5. Statistical Summary of Test Well

Statistical Parameter	Formation Pressure	TVD	Bit Size	Porosity	Bulk Density	Resistivity	ROP	WOB	RPM	Torque	SPP	Flow In	FL Temp	Gas Level
	(Psi)	(Ft)	(in)	(%)	(gm/cc)	(ohm)	M/hr.)	(K. lb.)		(lb. f)	(psi)	(GPM)	(C)	(PPM)
Maximum	4765.28	10830.19	8.5	0.38	2.87	2000	119.4	43.19	151.95	13236.36	3077.56	519.84	63.27	73251
Minimum	3572.22	7765.70	8.5	0.01	2.23	0.41	3.56	2.4	9.45	2283.64	1502.50	370.64	34.68	2236
Range	1193.06	3064.49	0	0.37	0.64	1999.59	115.84	41.19	142.50	10952.72	1575.07	149.20	28.59	71015
Mean	4238.16	9312.50	8.5	0.193	2.58	31.22	29.18	24.87	125.82	7358.85	2150.62	443.62	48.99	7697.88
Median	4287.21	9320.03	8.5	0.18	2.58	2.04	26.91	25.36	129.08	7256	2204.81	441.16	44.14	6057.82
Standard Deviation	348.99	881.20	0	0.089	0.090	222.73	13.75	8.60	16.86	2331.32	439.60	36.61	9.06	5701.58
1st Q	3935.85	8556.2	8.5	0.14	2.53	0.97	20.10	17.58	117.99	5342.55	1741.95	405.04	41.93	4852
3rd Q	4553.43	10073.20	8.5	0.27	2.64	4.82	37.28	32.14	139.02	9230.55	2465.23	474.32	60.21	8631.88

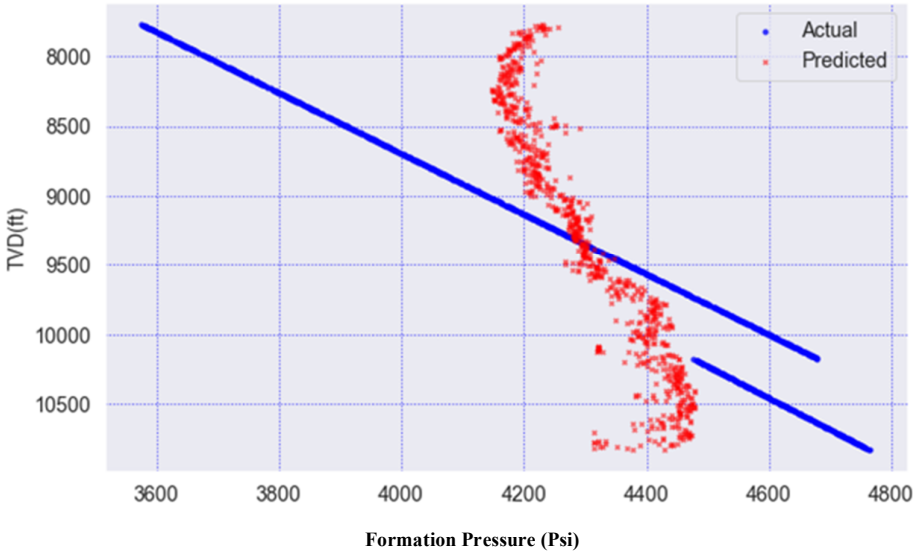

Figure 13. Actual and Predicted Formation Pressure Vs. Depth for KNN model - well X

An additional tool is used to measure the effect of each input on the output. This tool is SHAP (SHapley Additive exPlanations), which has corresponding values. SHAP value is a method to explain the outputs of the ML models. It uses a game-theoretic approach that measures each individual feature's contribution to the final outcome and is relative to the model's expected value. In machine learning, each feature is assigned an importance value representing its contribution to the model's output [32]. In this research, we use SHAP Decision Plots to show how the model arrives at the predictions. Figure 16 shows the SHAP Decision plot of the RF Model with the plot centered on the X-axis around the Explainer expected value, which is equal to 4780.58 psi, while the Y-axis has the model's input features ordered from top to bottom based on importance and contribution (feature's importance is based on the observations plotted). Each line represents an

observation that strikes the X-axis at the top at the corresponding expected value. Figure 17 shows the observation plot and the effect of each feature on the prediction. It can be seen that the depth has the greatest effect on the prediction, where E[F(x)] is the explainer's expected value and f(x) is the predicted value of the observation. Also, each feature has the corresponding SHAP value next to it and the contributing based on the importance on the plot.

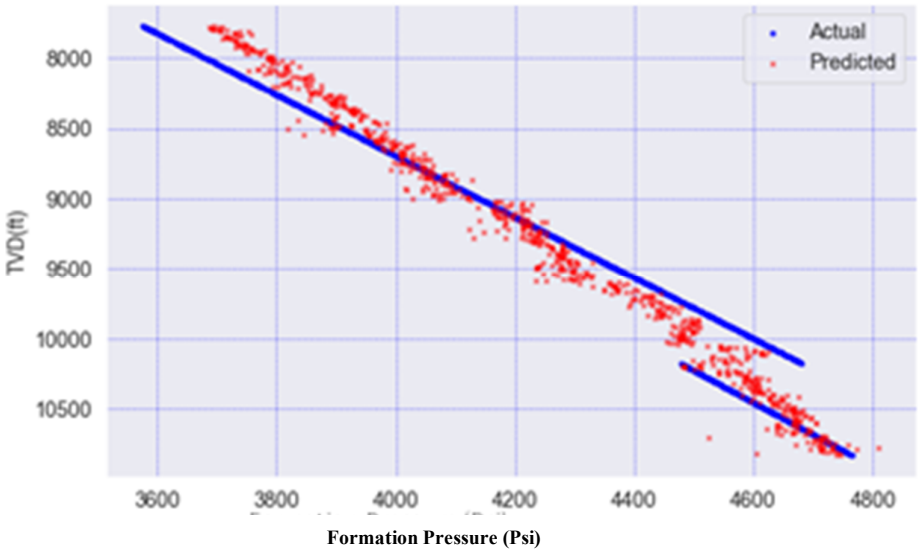

Figure 14. Actual and Predicted Formation Pressure Vs. Depth for RF model – well X

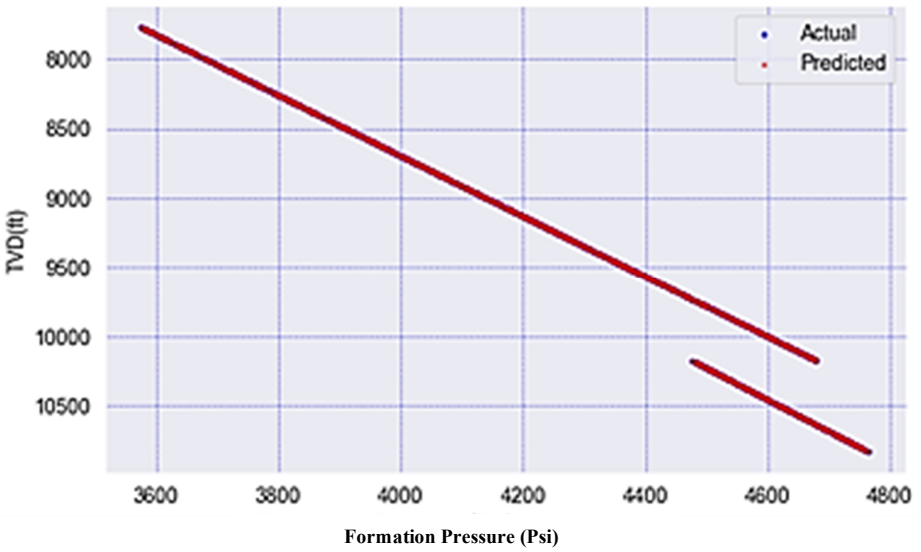

Figure 15. Actual and Predicted Formation Pressure Vs. Depth for XGB model - well X

5.2. Deployment and User Interface Program

Streamlit is used for deploying the Random Forest machine learning model as a web service. Figure 18 shows the program interface on **Streamlit.** The interface program has been evaluated with a different well **Y** to measure its credibility with 196 points and found the accuracy of results to be 95%. Table 6 shows the statistical summary of the data for well **Y**.

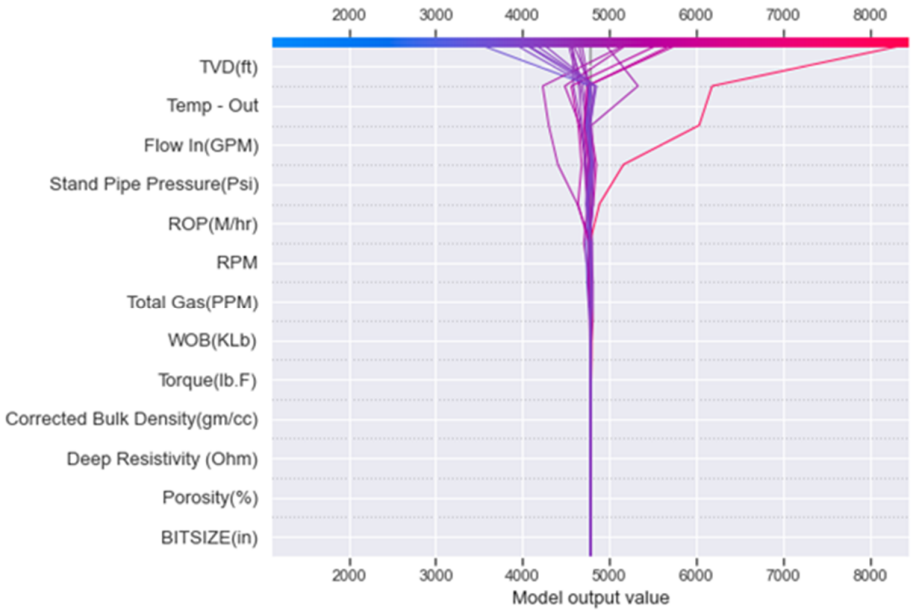

Figure 16. Decision plot showing observations and predicted values based on the feature importance and SHAP Value

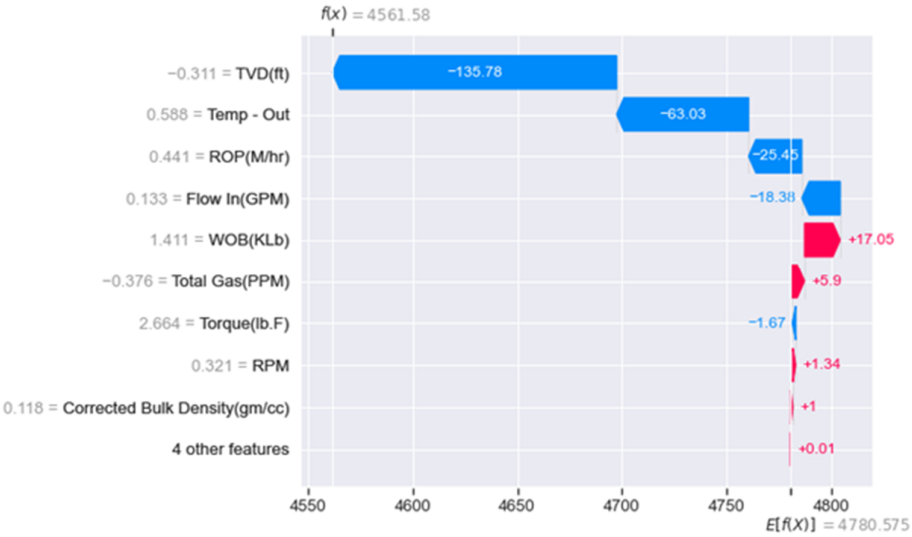

Figure 17. Sample of the Observation from Decision plot

Table 6 Statistical summary for the test well Y

Statistical Parameter	Formation Pressure	TVD	Bit Size	Porosity	Bulk Density	Resistivity	ROP	WOB	RPM	Torque	SPP	Flow In	FL Temp	Gas Level
	(Psi)	(Ft)	(in)	(%)	(gm/cc)	(ohm)	M/hr.)	(K. lb.)		(lb. f)	(psi)	(GPM)	(C)	(PPM)
Maximum	4522.87	9961.62	8.5	0.46	2.82	401.91	117.26	55.07	128.40	14680	3532.94	572.87	37.23	12601.16
Minimum	2257.27	9340.81	8.5	0.022	2.27	0.72	4.68	8.35	70	903.42	2522.51	528.10	22.51	2250.55
Range	2265.60	620.82	0	0.44	0.55	401.19	112.57	46.72	58.40	13776.57	1010.43	44.77	14.72	10350.61
Mean	3898.61	9651.06	8.5	0.21	2.61	27.02	49.66	42.77	102.51	11424.84	3100.83	551.74	26.34	7332.04
Median	4379.80	9650.99	8.5	0.21	2.61	2.92	49.97	44.07	102.82	11475	2986.15	569.96	22.76	7568.16
Standard Deviation	917.04	180.14	0	0.099	0.099	79.19	16.90	7.03	5.83	1771.88	293.60	20.42	5.25	1968.67
1st Q	4308.32	9495.85	8.5	0.13	2.56	1.72	39.91	39.91	101.30	10577.50	2830.28	531.04	22.67	6003.08
3rd Q	4451.32	9806.18	8.5	0.27	2.68	13.46	59.82	46.95	104.94	12547.50	3391.94	571.41	31.32	8701.36

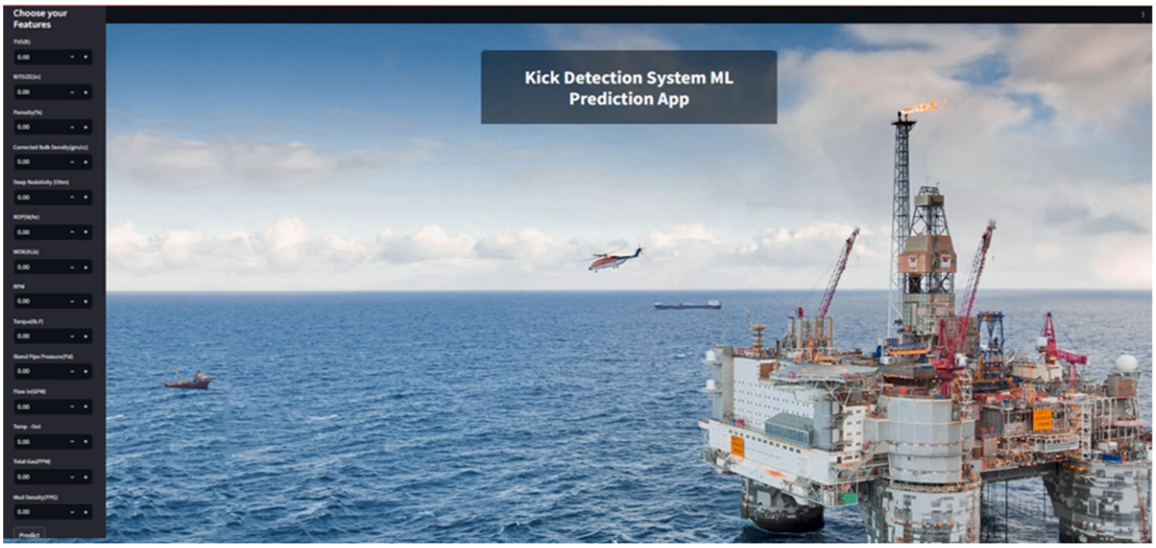

Figure 18. Program interface showing input variables to the left.

6. Conclusions

Conventional kick detection methods take a long time to record the kick, and this leads to an increase in the kick size and makes it harder to regain well control. Also, this model shows higher accuracy and fast response than some of the developed models. This research used the benefit of machine learning to recognize the kick before it enters the wellbore by predicting the abnormal formation pressure. In conclusion:

- The ML tools depict a great advantage over conventional methods as it detects the abnormal formation pressure and the possible kick in place at the moment the bit drills through the formation.
- This ML Model shows higher accuracy than other ML Models in predicting formation pressure and kick.
- Since the parameters entered to the model are taken from the instantaneous readings of the drilling, so, no delay of formation pressure and kick detection like other ML Models.
- The proposed models lead to enhance the kick performance indicators by decreasing the kick detection volume and kick response time.
- The KNN model shows low R^2 and high RMSE values with a greater scatter of data.
- The XGB model shows overfitting of the data in the training stage and is not stable through the test, and validation stages.
- The Random Forest model is found to be the best among the three models, with average R^2 = 0.9638 and RMSE = 12.86.
- The Interface program was evaluated and showed an accuracy of 95%.
- Even with computers with high computational power, caution must be considered to avoid making a non-required, non-valid correlation between parameters as computers do not understand the drilling operations.

We recommend that the current model needs to be continuously fed with data, trained, and tested to increase its effectiveness and widen its area of coverage.

Conflict of Interest

we certify that we have no commercial associations (e.g., consultancies, stock ownership, equity interests, patent-licensing arrangements, etc.) that might pose a conflict of interest in connection with the submitted article, except as disclosed on a separate attachment. All funding sources supporting the work and all institutional or corporate affiliations of ours are acknowledged in a footnote.

Funding Declaration

The authors declare No funding was received.

References

[1]. Schools, A. D. (2002). Well control for the rig-site drilling team. *Training Manual*.

[2]. President Commission. (2011). National Commission on the BP Deepwater Horizon Oil Spill and Offshore Drilling: Deepwater. *The Gulf Oil Disaster and the Future of Offshore Drilling*.

[3]. Sætren, T. G. (2007). *Offshore blow-out accidents: an analysis of causes of vulnerability exposing technological systems to accidents* (Master's thesis).

[4]. A. O. Erete, E. E. Okoro, E. Ekeinde, and A. Dosunmu, "A New Approach To Kick Detection and Diagnosis in Drilling Operation," International Journal of Advanced Research in Education & Technology (IJARET), vol. 3, no. 2, pp. 151–156, 2016.

[5]. Magana-Mora, A., Affleck, M., Ibrahim, M., Makowski, G., Kapoor, H., Otalvora, W. C., ... & Gooneratne, C. P. (2021). Well control space out: A deep-learning approach for the optimization of drilling safety operations. *IEEE Access*, *9*, 76479-76492.

[6]. Sircar, A., Yadav, K., Rayavarapu, K., Bist, N., & Oza, H. (2021). Application of machine learning and artificial intelligence in oil and gas industry. *Petroleum Research*, *6*(4), 379-391.

[7]. Muojeke, S., Venkatesan, R., & Khan, F. (2020). Supervised data-driven approach to early kick detection during drilling operation. *Journal of Petroleum Science and Engineering*, *192*, 107324.

[8]. Khamis, Y. E., El-Rammah, S. G., & Salem, A. M. (2023). Rate of penetration prediction in drilling operation in oil and gas wells by k-nearest neighbors and multi-layer perceptron algorithms. *Journal of Mining and Environment*, *14*(3), 755-770.

[9]. H. Rabia, Well Engineering & Construction. Entrac Consulting Limited, 2002.

[10]. Chevron Energy Technology Company (CETC), Drilling Well Control Guide. 2006.

[11]. Aramco, S. (2002). Well Control Manual, Drilling and Workover.

[12]. Ahmed, M. A., Hegab, O. A., & Sabry, A. (2016). Early detection enhancement of the kick and near-balance drilling using mud logging warning sign. *Egyptian journal of basic and applied sciences*, *3*(1), 85-93.

[13]. Tost, B., Rose, K., Aminzadeh, F., Ante, M. A., & Huerta, N. (2016). *Kick detection at the bit: Early detection via low cost monitoring* (No. NETL-TRS-2-2016). National Energy Technology Laboratory (NETL), Pittsburgh, PA, Morgantown, WV (United States).

[14]. American Petroleum Institute (API), API Standard 53, Well Control Equipment system for Drilling Wells, 5th ed. API Publishing Services, 2018.

[15]. H. Abdul-Ameer, "Machine Learning Methods for Kick Detection (Doctoral Dissertation)," University of Calgary, Calgary, Canada, 2023. doi: https://dx.doi.org/10.11575/PRISM/40680.

[16]. Nayeem, A. A., Venkatesan, R., & Khan, F. (2016). Monitoring of down-hole parameters for early kick detection. *Journal of Loss Prevention in the Process Industries*, *40*, 43-54.

[17]. Islam, R., Khan, F., & Venkatesan, R. (2017). Real time risk analysis of kick detection: testing and validation. *Reliability Engineering & System Safety*, *161*, 25-37.

[18]. Faraj, A. K., & Hussein, H. A. H. A. (2022). Calculation Pore Pressure Utilized Two Methods/Case Study of Zubair Oil Field. *Texas Journal of Engineering and Technology*, *11*, 1-6.

[19]. Nelli, F. (2018). Python data analytics with Pandas, NumPy, and Matplotlib.

[20]. Flach, P. (2012). *Machine learning: the art and science of algorithms that make sense of data*. Cambridge University Press.

[21]. Osarogiagbon, A., Muojeke, S., Venkatesan, R., Khan, F., & Gillard, P. (2020). A new methodology for kick detection during petroleum drilling using long short-term memory recurrent neural network. *Process Safety and Environmental Protection*, *142*, 126-137.

[22]. Fjetland, A. K. (2019). *Kick Detection During Offshore Drilling Using Artificial Intelligence* (Master's thesis, Universitetet i Agder; University of Agder).

[23]. Grus, J. (2019). *Data science from scratch: first principles with python*. O'Reilly Media.

[24]. Wu, X., Kumar, V., Ross Quinlan, J., Ghosh, J., Yang, Q., Motoda, H., ... & Steinberg, D. (2008). Top 10 algorithms in data mining. *Knowledge and information systems*, *14*, 1-37.

[25]. Mining, W. I. D. (2006). *Introduction to data mining* (pp. 2-12). New Jersey: Pearson Education, Inc.

[26]. Breiman, L. (2001). Random forests. *Machine learning*, *45*, 5-32.

[27]. Bentlemsan, M., Zemouri, E. T., Bouchaffra, D., Yahya-Zoubir, B., & Ferroudji, K. (2014, January). Random forest and filter bank common spatial patterns for EEG-based motor imagery classification. In *2014 5th International conference on intelligent systems, modelling and simulation* (pp. 235-238). IEEE.

[28]. Blakely, L., Reno, M. J., & Broderick, R. J. (2018, February). Decision tree ensemble machine learning for rapid QSTS simulations. In 2018 IEEE Power & Energy Society Innovative Smart Grid Technologies Conference (ISGT) (pp. 1-5). IEEE.

[29]. Chen, T., & Guestrin, C. (2016, August). Xgboost: A scalable tree boosting system. In *Proceedings of the 22nd acm sigkdd international conference on knowledge discovery and data mining* (pp. 785-794).

[30]. Malik, S., Harode, R., & Kunwar, A. (2020). XGBoost: A deep dive into boosting. *Simon Fraser University*, 1-21.

[31]. Singh, P. (2021). Deploy machine learning models to production. *Cham, Switzerland: Springer*.

[32]. Mosca, E., Szigeti, F., Tragianni, S., Gallagher, D., & Groh, G. (2022, October). SHAP-based explanation methods: a review for NLP interpretability. In *Proceedings of the 29th international conference on computational linguistics* (pp. 4593-4603).

مدل پیشنهادی جدید برای تشخیص زود هنگام ضربه در عملیات حفاری با استفاده از یادگیری ماشینی

مصطفی یاسر الگیندی[1,2*]، احمد نوح[3] و علی وهبه[2]

۱- مهندس خدمات حفاری و چاه، بخش خدمات حفاری و چاه، شرکت نفت بدر الدین (BAPETCO)، قاهره، مصر

۲- گروه مهندسی نفت، دانشکده مهندسی نفت و معدن، دانشگاه سوئز، سوئز، مصر

۳- مؤسسه تحقیقات نفت مصر (EPRI)، شهر نصر، قاهره، مصر

ارسال ۲۰۲۴/۰۷/۱۸، پذیرش ۲۰۲۴/۱۱/۲۰

* نویسنده مسئول مکاتبات: mustafa.muel@pme.suezuni.edu.eg

چکیده:

نظارت، تشخیص و کنترل ضربه، عناصر کلیدی برای اطمینان از عملیات حفاری ایمن و جلوگیری از حوادث انفجاری فاجعه‌بار است که می‌تواند باعث از دست دادن جان، تجهیزات و آسیب‌های محیطی شود. سیستم‌های تشخیص لگد معمولی مانند توتالایزر حجم گودال و حسگرهای جریان ورودی/خروجی ضربه را پس از ثبت مقدار زیادی هجوم روی سطح شناسایی می‌کنند. بنابراین، هدف ما این است که لگد را قبل از ورود به چاه با تشخیص فشار تشکیل غیرعادی پس از نفوذ بیت به سنگ تشخیص دهیم. این مقاله یک مدل یادگیری ماشین جدید را به عنوان یک راه حل جایگزین با استفاده از پارامترهای حفاری میدانی مانند عمق عمودی واقعی، تخلخل، چگالی ظاهری، مقاومت، نرخ نفوذ، وزن روی بیت، چرخش در دقیقه، گشتاور، فشار لوله ایستاده، سرعت جریان، خط جریان پیشنهاد می‌کند. دما و سطح گاز مدل‌های مبتنی بر داده با استفاده از سه الگوریتم مجزا توسعه داده شدند: K-Nearest Neighbor، Random Forest و XG Boost 6022 نقطه داده میدانی برای فرآیندهای آموزش، آزمایش و اعتبار سنجی تقسیم شدند. به طور متوسط، مدل با استفاده از الگوریتم جنگل تصادفی با مقادیر میانگین مربعات خطای ریشه و مقادیر ضریب تعیین به ترتیب ۱۲/۸۶۸ و ۰/۹۶۳۸، بیشترین دقت را در پیش‌بینی فشار سازند نشان داد. ابزار Streamlit Deployment برای ایجاد یک برنامه رابط کاربری برای تسهیل فرآیند پیش‌بینی استفاده شد. این برنامه با استفاده از ۱۹۶ نقطه داده میدانی آزمایش شد و دقت بالای ۹۵ درصد را ثبت کرد.

کلمات کلیدی: تشخیص زودهنگام ضربه، یادگیری ماشین، پارامترهای حفاری، فشار تشکیل غیرعادی.